

condition, most propitious to crack initiation and consequently the break of the tested wire under fretting fatigue [8]. A micrograph of the resulting fretting mark of both uniaxial and biaxial tests is shown in Fig. 6. In both cases, the fretting fatigue crack was initiated in the contact area. A clear mark is observed in the center of the contact area where no relative motion between wire and pads would occur, surrounded by a dark mark representing the micro slip area. This observation is clearer on the uniaxial tested wires than on the biaxial ones and that can be explained by the effect of the alternating bending in biaxial tests which expands the contact area and consequently enlarges the slipping mark to the detriment of the sticking mark. The alternating bending effect is also noticed by comparing the geometry of the contact area in both types of tests. It can be seen that the contact area in the uniaxial tests has an elliptical shape while in the biaxial ones it is almost linear and more extended.

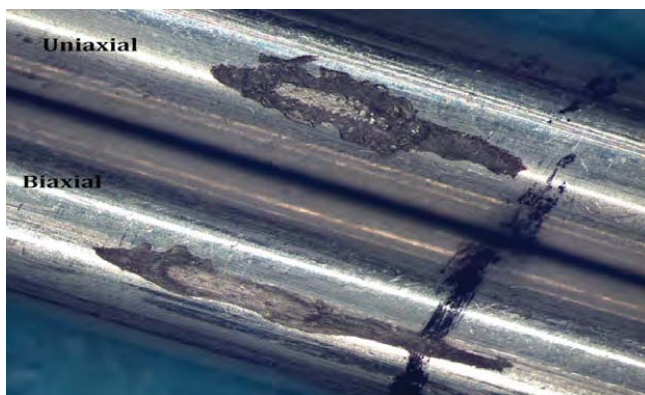


Fig.6. Fretting fatigue marks under uniaxial and biaxial loading.

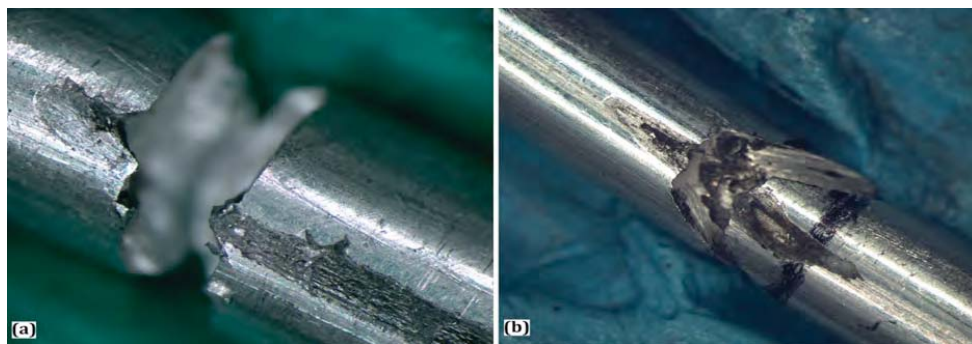


Fig.7. Fretting fatigue breaks in (a) biaxial and (b) uniaxial test.

Fig. 7 is a micrograph of fretting breaks that occurred respectively in a biaxial and a uniaxial test. In the first case, the breaking point is near the last point of contact while in the second one, it is virtually located in the center of the contact area. When comparing the cracking plan of both test types, we notice two different fracture patterns. For the uniaxial tests, the cracking plane is inclined about 45° to the wire axis which confirms the presence of the mixed stick-slip condition. However, in the case of the biaxial tests, the break occurs along a plane parallel to the section of the wire thus proving the dominance of the partial slip regime [10]. In fact, the tangential force can be easily controlled in the uniaxial tests to establish the mixed fretting regime, which is not the case for the biaxial ones where the alternating bending induces an additional component in the tangential force which is difficult to control.

5.2 Uniaxial tests results

The results of the uniaxial tests are presented in table 3. During these tests, the estimated micro-sliding was always in the range of 5 to $50\mu\text{m}$, the typical values resulting in fretting fatigue [11]. At a very high alternating stress level ($\sigma_a = \pm 56\text{MPa}$), all recorded breaks were due to plain fatigue and were located outside the contact area, at the attachment point of the wire to the actuator A_2 . However, at moderate levels of the alternating stress ($\sigma_a = \pm 43\text{MPa}$ and $\sigma_a = \pm 35\text{MPa}$), most of the breaks were in the contact area between the wire and the pads and were caused by fretting fatigue. At the lowest alternating stress level ($\sigma_a = \pm 25\text{MPa}$), tests reached the fixed lifetime limit without recording a

break. The fatigue life of the wire is slightly affected by the normal contact force. At high amplitude, the decrease of this force results in a decrease in the number of cycles to failure, whereas near the endurance limit the variation of this force has practically no effect on the fatigue life.

Table 3. Results of the uniaxial tests.

Test number	Number of cycles	Breaking position	Breaking cause	Q (N)	δ (μm)
1	1.760.991	At the attachment point A ₂	Plain fatigue	90	16
2	1.439.617	At the attachment point A ₂	Plain fatigue	95	17
3	735.500	At the attachment point A ₂	Plain fatigue	93	17
4	3.209.610	In the contact area	Fretting fatigue	92	16
5	7.544.760	At the attachment point A ₂	Plain fatigue	95	17
6	2.634.397	In the contact area	Fretting fatigue	42	8
7	2.418.054	In the contact area	Fretting fatigue	50	9
8	6.933.267	In the contact area	Fretting fatigue	112	20
9	7.143.537	At the attachment point A ₂	Plain fatigue	107	19
10	7.356.070	In the contact area	Fretting fatigue	112	20
11	20.000.000	No break		109	20
12	20.000.000	No break		40	7
13	20.000.000	No break		32	6

5.3 Biaxial tests results

Biaxial tests were also performed for the loading configuration identified in table 2 earlier. As presented in table 4, the majority of the breaks were due to fretting fatigue and were in the contact area between the tested specimen and the pads. Fig.8 illustrates the results of both uniaxial and biaxial tests as S-N curves. At this stage of the experimental study, the results obtained are not sufficient to fully compare both types of tests in terms of fatigue life. However, it can be observed that the setup allows getting some fretting fatigue failures at high stress amplitudes for biaxial loading, whereas early plain fatigue failures are recorded when performing similar uniaxial tests. Furthermore, the relation between the number of cycles to failure and the alternating stress appears to be different for the uniaxial and biaxial tests.

Table 4. Results of the biaxial tests.

Test number	Number of cycles	Breaking position	Breaking cause
14	3.845.950	In the contact area	Fretting fatigue
15	2.910.136	In the contact area	Fretting fatigue
16	3.112.426	In the contact area	Fretting fatigue
17	4.092.373	In the contact area	Fretting fatigue
18	7.449.855	At the attachment point A ₂	Plain fatigue

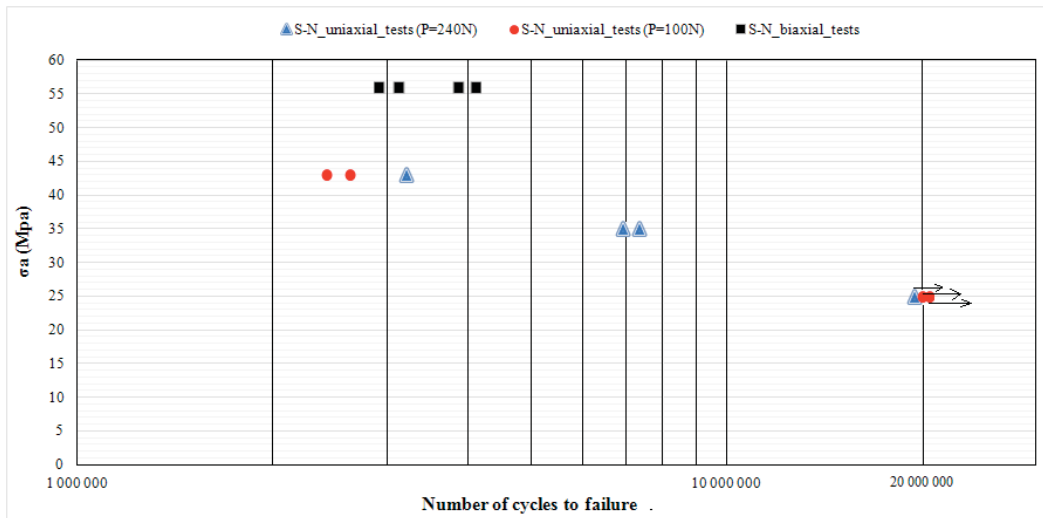


Fig. 8. Fatigue data of the uniaxial and the biaxial tests.

6 Conclusions

The design of a biaxial fretting fatigue test bench has been presented in this paper. The results of the preliminary tests have shown that this experimental setup allows performing both uniaxial and biaxial loading tests. At very high levels of alternating stress, the developed test bench enables to perform biaxial tests better than uniaxial ones. The performance of the developed device has been verified through the creation of fretting marks leading to fretting fatigue failure. Some breaks have occurred outside the contact area, at the attachment point of the wire to the axial actuator, which requires improving the clamping system in order to minimize the stress level at both ends of the tested wires. A wide variety of fretting fatigue tests representing strand damages occurring at the conductor-clamp and the inter-wire contact points and involving different parameters such as the normal contact force, the alternating tension and the alternating bending can be reproduced in the presented test bench.

References

1. IEC 62568 International Standard, *Overhead lines – Method for fatigue testing of conductors* (2015)
2. L. Cloutier, S. Goudreau, A. Cardou, *EPRI Transmission Line Reference Book – Wind Induced Conductor Motion*, 3.1-3.56 (2006)
3. S. Lalonde, R. Guilbault, S. Langlois, Numerical analysis of ACSR conductor-clamp systems undergoing wind-induced cyclic loads, *IEEE Trans. on Pow. Deli.*, **33**: 1518-1526 (2018)
4. F. Lévesque, S. Goudreau, A. Cardou, L. Cloutier, Strain measurements on ACSR conductors during fatigue tests I- Experimental method and data, *IEEE Trans. on Pow. Deli.*, **25**: 2825-2834 (2010)
5. P. U. Wittkowsky, P. R. Birch, J. Dominguez, S. Suresh, An apparatus for quantitative fretting fatigue testing, *Fatigue Fract. Eng. Mater. Struct.*, **22**: 307-320 (1999)
6. J. Lanteigne, L. Cloutier, A. Cardou, *Fatigue life of aluminum wires in all aluminum and ACSR conductors*, CEA, Canada (1986)
7. S. Lalonde, *Stratégie de modélisation 3D des solides toronnés appliquée à l'étude de la fatigue des conducteurs de lignes de transport d'énergie électrique*, Université de Sherbrooke, Canada (2017)
8. O. Vingsbo, S. Söderberg, On fretting maps, *Wear*, **126**: 131-147 (1988)
9. Z. R. Zhou, L. Vincent, Mixed fretting regime, *Wear*, **181-183**: 531-536 (1995)
10. Z. R. Zhou, A. Cardou, S. Goudreau, M. Fiset, Fundamental investigations of electrical conductor fretting fatigue, *Trib. Inter.*, **29**: 221-232 (1996)
11. S. Suresh, *Fatigue of materials*, 679 (1998).